







Finite Element Analysis of Stress Distribution in Underground Galleries with Varying Dimensions

Mustafa Emre Yetkin^{*}, Muharrem Kemal Özfırat[†], Hayati Yenice[‡], Turgay Onargan[§]

Faculty of Engineering, Mining Engineering Department, Dokuz Eylül University, Izmir 35390, Turkey

Corresponding Author Email: mustafa.yetkin@deu.edu.tr

Copyright: ©2024 The authors. This article is published by IETA and is licensed under the CC BY 4.0 license (<http://creativecommons.org/licenses/by/4.0/>).

<https://doi.org/10.18280/eesrj.110102>

ABSTRACT

Received: 21 November 2023

Revised: 11 January 2024

Accepted: 18 January 2024

Available online: 31 March 2024

Keywords:

finite element method, stress distribution, underground galleries, mining

In underground mining, stresses within the rock mass are initially in a state of equilibrium. Excavation disrupts this balance, necessitating the establishment of a new stress equilibrium. The reinforcement of mine galleries is contingent upon an understanding of the geomechanical properties of the rock mass. Furthermore, the dimensions of these galleries significantly influence the distribution of stresses around them. This study investigates the normal and horizontal stresses surrounding galleries of varying dimensions, excavated under identical rock mass conditions. The findings facilitate the recommendation of optimal gallery sizes that minimize stress concentrations. Consequently, these recommendations are instrumental in enabling the selection of gallery sizes that enhance mining safety and ensure sustainable production.

1. INTRODUCTION

The design and execution of mine galleries are pivotal to mining operations, underpinning critical functions such as occupational safety, ventilation, water management, and the movement of personnel and materials. Appropriately dimensioned galleries are imperative for a productive and secure work environment. The determination of these dimensions is influenced by a myriad of factors, including underground stress conditions, the transportation demands for heavy machinery, and the operational requirements for personnel and equipment. Informed selection of gallery dimensions, guided by these parameters, is essential for optimizing occupational safety and operational efficiency.

Historically, research efforts have been directed toward modeling stresses and failure potentials associated with circular cross-section tunnels within rock masses. The response of these underground structures to static loads has been extensively examined through numerical simulations [1-6].

In the present study, gallery models measuring 4×4 meters and 5×5 meters were developed within an identical geological setting. The selection process for the gallery dimensions was informed by the strength characteristics of the local rock mass and the prevalent dimensions within existing mining operations. Consequently, dimensions of 4×4 and 5×5 meters were identified as optimal for further investigation. The stress profiles, both vertical and horizontal, associated with these gallery dimensions were scrutinized. Initially, a representative model of the field was constructed, enabling the estimation of stress distributions. Subsequently, the computed stress values were imposed upon the gallery models to determine the stress patterns that would manifest around these structures. Based on

the stress distributions obtained, recommendations pertaining to the most advantageous gallery dimensions were formulated.

2. CREATION OF THE MODEL

The data of the rock material considered in the created field model are provided in Table 1. The underground quarry under investigation in this study is located 70 km east of İzmir and 15 km northwest of Bayındır.

Table 1. Data related to rock material [7]

	Rock Material	Deadrock
Uniaxial Compressive Strength	UCS (MPa)	35.67
Geological Strength Index	GSI	60
Rock Mass Constant	mi	20
Density	γ (t/m ³)	2.7

During the creation of the field model, a depth of 90 meters from the surface was considered for excavating the galleries. In the subsequent stage, using the rock material properties provided in Table 1 and considering the depth, the parameters related to the rock mass were calculated using RocData software [8]. The process of obtaining the rock mass data is illustrated in Figure 1.

The data related to the rock mass calculated using the RocData software are provided in Table 2.

The horizontal and vertical stress values that will occur at a working depth of 90 meters under the selected rock mass conditions, considering the Poisson's ratio of the dominant rock structure in the field, have been calculated using the following equations [9]:

$$\sigma_h = k \cdot \sigma_v \quad (1)$$

$$k = 0,25 + 7 \cdot E \cdot (0,001 + 1/z) \quad (2)$$

Here is a brief explanation of the variables: σ_v : Vertical stress in megapascals (MPa); σ_h : Horizontal stress in megapascals (MPa); k : Ratio of horizontal stress to vertical stress (no units); E : Average modulus of elasticity of the rock mass in the vertical direction up to the working depth in gigapascals (GPa); z : Working depth in meters (m).

The vertical stress at a working depth of 90 m was calculated as 2.33 MPa using Eq. (1). Considering the rock mass properties given in Table 2 and the calculated coefficient k as 0.84 based on the rock mass's modulus of elasticity and depth (Eq. (2)), the expected horizontal stress in the field was calculated as 1.96 MPa. The calculated coefficient k was incorporated into the field model, ensuring an accurate representation of stress conditions within the rock mass environment where the galleries will be excavated. Field models with dimensions of 4x4 meters and 5x5 meters were

created using Phase2D software [10]. A visual representation of the models is provided in Figure 2.

After entering the data the models, the models were run, and normal and horizontal stresses around the galleries were calculated for different gallery sizes. The stresses around the galleries with gallery sizes of 4x4 and 5x5 meters in the same rock mass environment are shown in Figure 3.

The calculated stress values are detailed in Table 3. Normal stresses occurring immediately above the gallery were measured along an approximately 14-meter line. The horizontal stress values on the right and left walls were recorded by measurements along an approximately 4-meter line. The measurements were conducted using measurement lines placed on models established within the software. These measurement lines are structures permitted to be generated by the software, allowing the user to obtain results of their desired intervals and types in the regions they pass through. The measurements were taken just above the gallery and on the side walls.

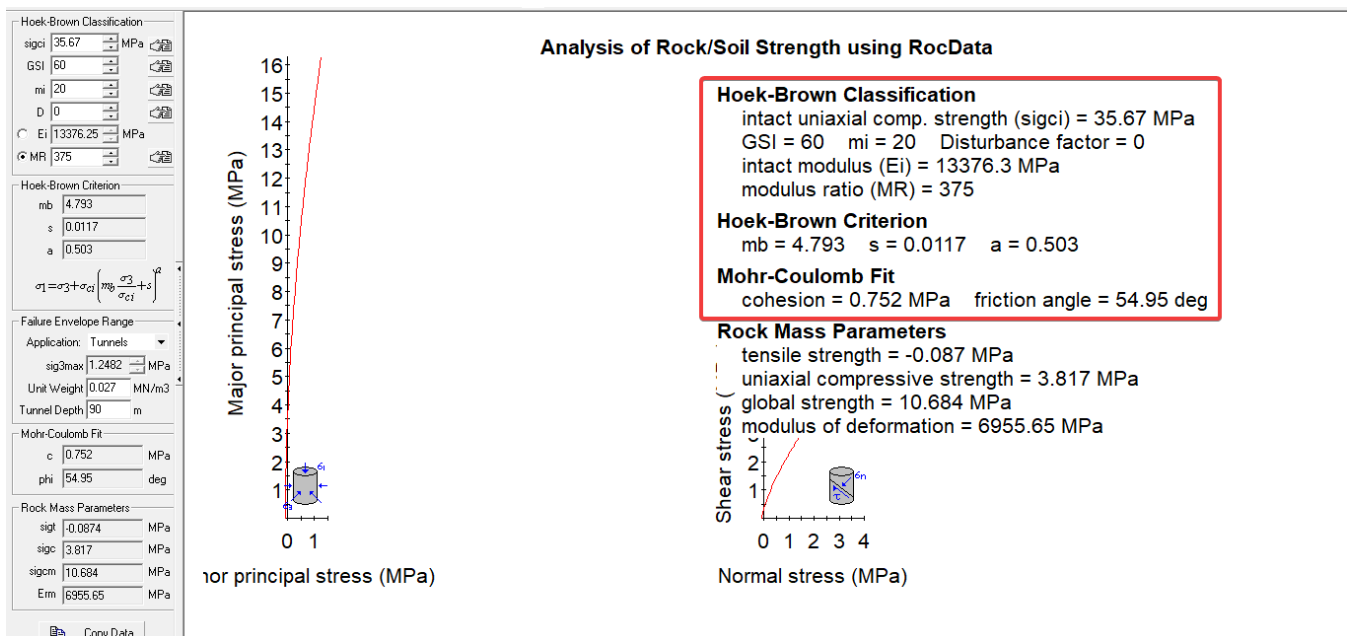


Figure 1. Obtaining rock mass data

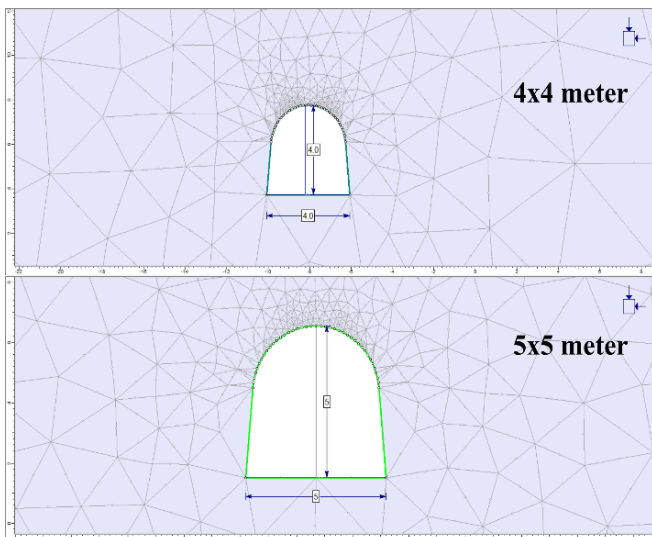


Figure 2. Different gallery size models

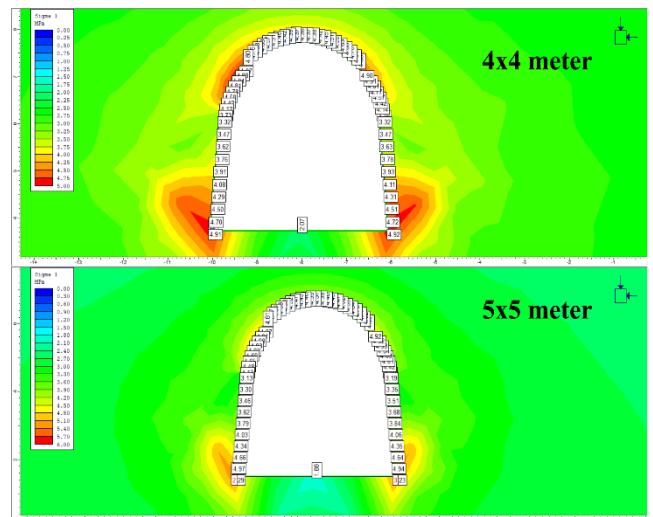


Figure 3. Normal stresses occurring around galleries of different sizes

Table 2. Rock mass data used in the model

Rock Mass		Deadrock
Elastic Modulus	E_M (MPa)	6955.650
Cohesion	C (MPa)	0.752
Tensile Strength	σ_t (MPa)	0.087
Internal Friction Angle	ϕ (Derece)	54.950
Density	γ (t/m ³)	2.700
Poisson's Ratio	ν	0.300

4.581	4.689
4.416	4.649
4.124	4.478
3.732	4.133
3.325	3.134
Mean	
4.498	4.555

Table 3. Normal and horizontal stresses occurring around galleries of different sizes

Gallery Size					
4×4 meter	5×5 meter	Horizontal Stresses (MPa)			
Top of Gallery		4×4 meter		5×5 meter	
Normal Stresses (MPa)		Left Wall	Right Wall	Left Wall	Right Wall
3.321	3.194	-0.325	-0.360	-0.183	-0.221
3.764	4.103	-0.201	-0.227	-0.102	-0.130
4.140	4.425	-0.077	-0.095	-0.021	-0.038
4.425	4.607	0.047	0.037	0.061	0.053
4.570	4.687	0.172	0.170	0.142	0.145
4.771	4.842	0.397	0.399	0.362	0.368
4.814	4.927	0.724	0.726	0.720	0.723
4.910	4.917	1.052	1.052	1.078	1.078
4.902	4.919	1.379	1.378	1.436	1.433
4.878	4.893	1.706	1.705	1.794	1.788
4.807	4.819	Mean			
4.755	4.770	0.487	0.479	0.529	0.520
4.679	4.698				
4.629	4.638				
4.578	4.580				
4.510	4.521				
4.452	4.469				
4.417	4.429				
4.384	4.396				
4.370	4.378				
4.361	4.371				
4.370	4.376				
4.385	4.397				
4.418	4.428				
4.456	4.468				
4.510	4.519				
4.574	4.578				
4.626	4.634				
4.677	4.685				
4.754	4.765				
4.804	4.815				
4.867	4.872				
4.881	4.911				
4.906	4.898				
4.807	4.929				
4.778	4.823				

3. CREATING GALLERY MODELS

In the context of modeling studies, two galleries have been designed with dimensions of 4×4 meters and 5×5 meters, both with a length of 20 meters. The gallery designs were created using the SpaceClaim [11] solid modeling software. A visual representation of the created models is provided in Figure 4. The purpose of creating three-dimensional models is to examine the normal stresses occurring in the third dimension along the z-axis around the galleries in more detail, as the models created in Phase2D software are two-dimensional.

After the creation stage of the gallery models, the models were transferred to the ANSYS [12] stress analysis program. The values provided in Table 2 were used as input parameters for the models in the ANSYS stress analysis program, thus ensuring that the model behaves like a real rock environment. The process of entering rock mass (Elastic Modulus, Density and Poisson's Ratio) data into the models is shown in Figure 5.

An image of the gallery models created in the ANSYS stress analysis program is provided in Figure 6.

The average normal stress values applied to the gallery models obtained from the Phase2D program and occurring on the gallery are as follows:

For the 4×4 meter gallery:

Average normal stress on the gallery: 4.498 MPa, Average horizontal stress on the right wall of the gallery: 0.479 MPa, Average horizontal stress on the left wall of the gallery: 0.487 Mpa.

For the 5×5 meter gallery:

Average normal stress on the gallery: 4.555 MPa, Average horizontal stress on the right wall of the gallery: 0.520 MPa, Average horizontal stress on the left wall of the gallery: 0.529 MPa.

These calculated stress values were applied regionally to the gallery models using the ANSYS stress analysis program. Before proceeding with stress analysis, the models were fixed to the ground and the effect of gravity was applied to the models. This was done to ensure that the models operate as accurately as possible. A visual representation of the models after applying the loads is provided in Figure 7.

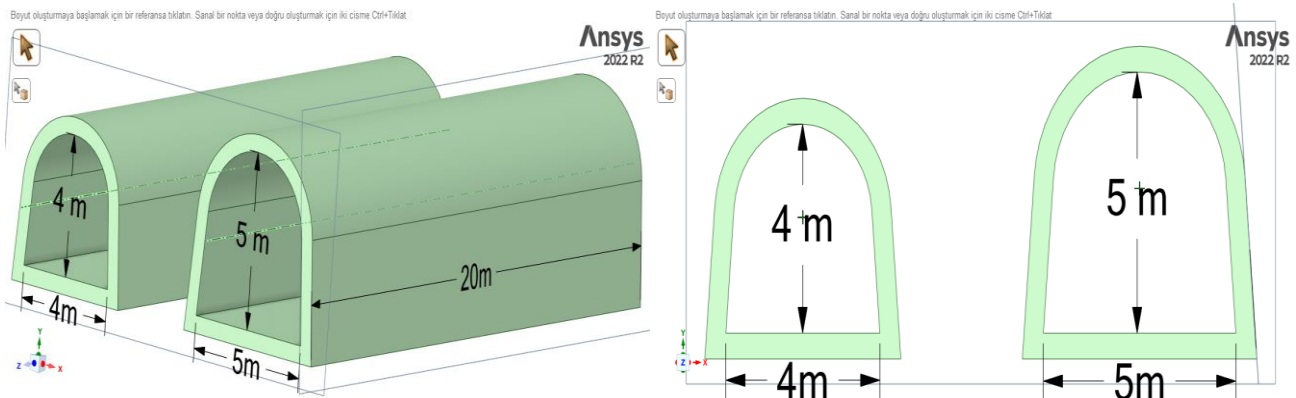


Figure 4. The created gallery models

Outline of Schematic A2: Engineering Data					
	A	B	C	D	E
1	Contents of Engineering Data		Source		Description
2	Material				
3	galeri 4x4				
4	galeri 5x5				
5	Structural Steel				Fatigue Data at zero mean stress comes from 1998 ASME BPV Code, Section 8, Div 2, Table 5 -110.1
*	Click here to add a new material				

Properties of Outline Row 4: galeri 5x5					
	A	B	C	D	E
1	Property	Value	Unit		
2	Material Field Variables	Table			
3	Density	2,7	g cm ⁻³		
4	Isotropic Elasticity				
5	Derive from	Young's Modulu...			
6	Young's Modulus	6955,7	MPa		
7	Poisson's Ratio	0,3			
8	Bulk Modulus	5,7964E+09	Pa		
9	Shear Modulus	2,6753E+09	Pa		

Figure 5. Entering input parameters into the gallery models

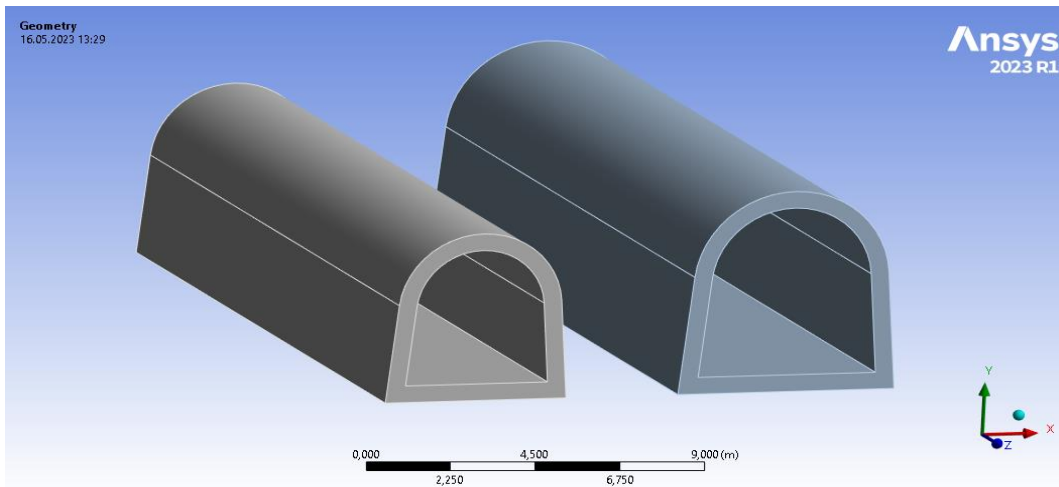


Figure 6. Gallery models in the 3rd dimension

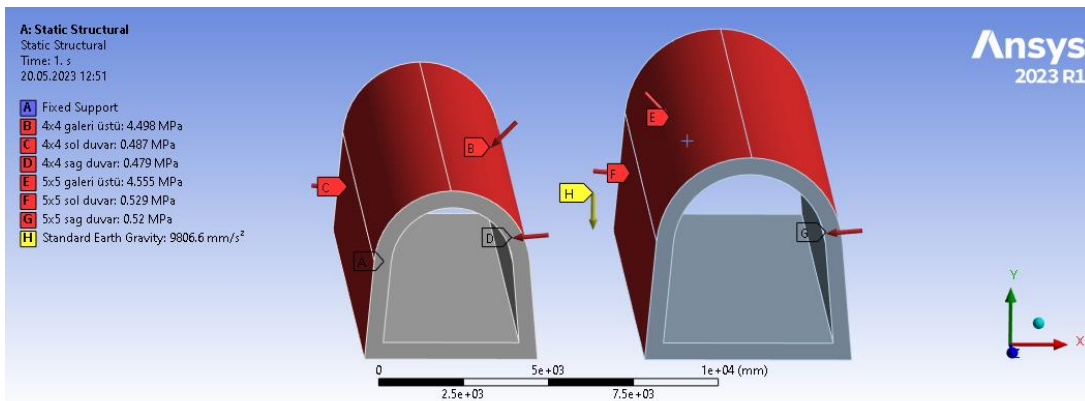


Figure 7. Application of normal (vertical) and horizontal (horizontal) stresses to gallery models

After completing these steps, the stress analysis process for the models was executed. An image showing the stress distribution around galleries of different sizes is provided in Figure 8. For the 4x4 meter gallery, the maximum vertical deformation was calculated to be 15.71 mm, whereas for the

5x5 meter gallery, it was calculated to be 19.85 mm. The distribution of deformations around the gallery is shown in Figure 9 and Figure 10. It is observed that the maximum deformation occurs in the central regions located just above the gallery in both cases.

In the ANSYS stress analysis, the combined and graphical representations of the normal stresses occurring around

galleries of different sizes are provided in Table 4 and Figure 11.

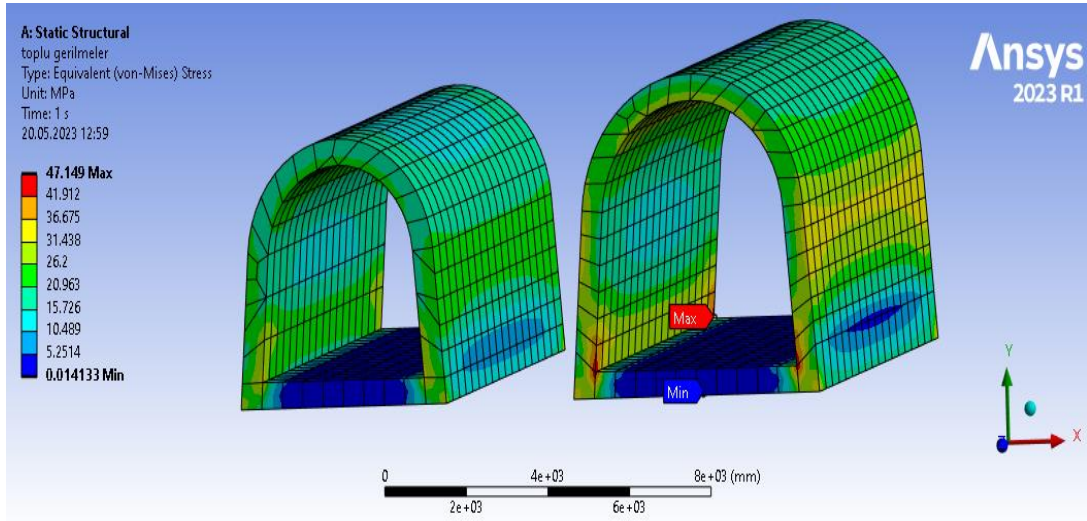


Figure 8. Stress distribution

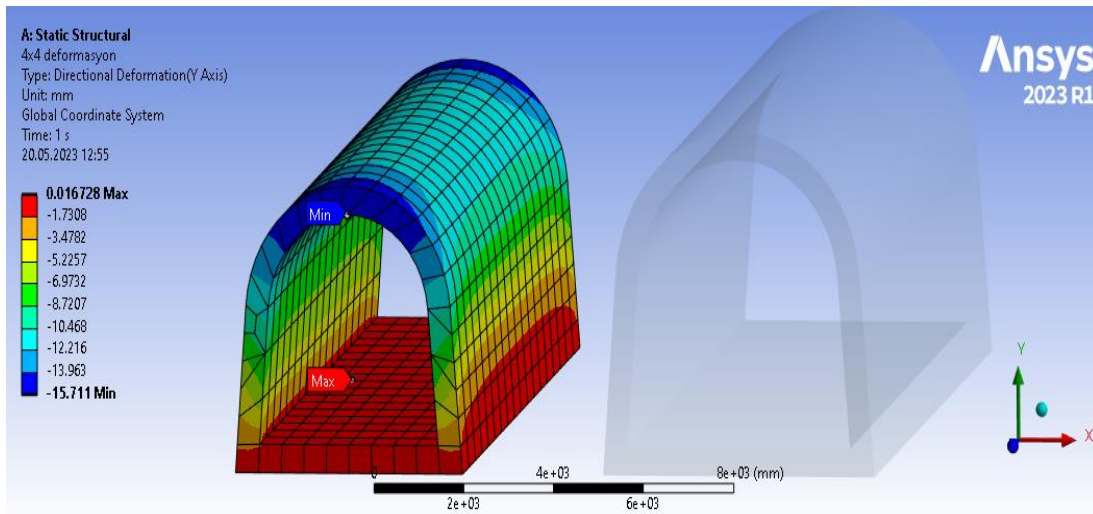


Figure 9. Vertical deformations occurring in the 4×4 meter gallery size

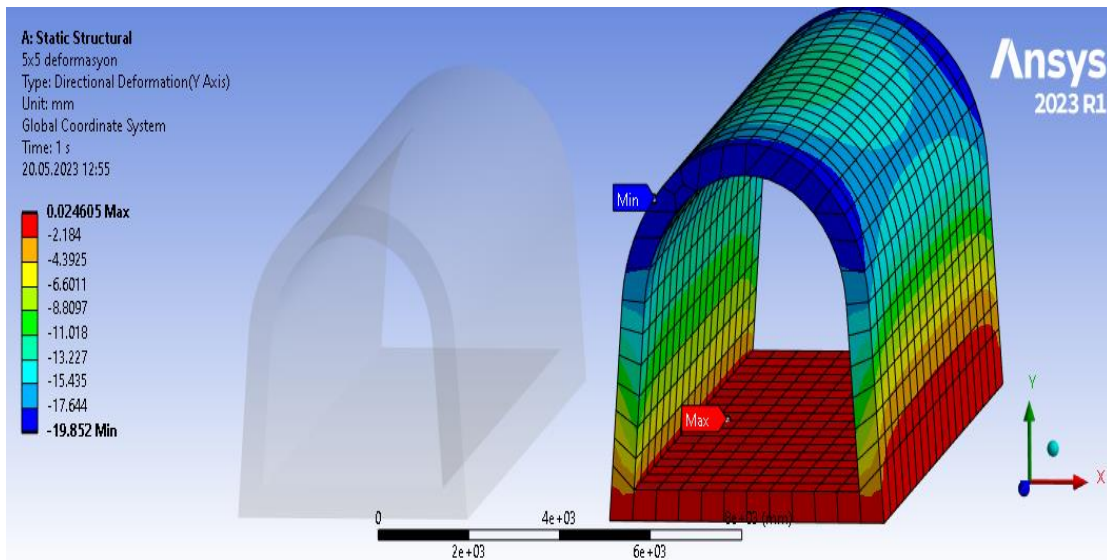


Figure 10. Vertical deformations occurring in the 5×5 meter gallery size

Table 4. Normal stresses occurring around galleries of different sizes

Gallery Size					
4x4 meter			5x5 meter		
Left Wall	Right Wall	Top of Gallery	Left Wall	Right Wall	Top of Gallery
24.973	24.991	16.322	27.986	28.089	17.075
24.869	24.890	16.444	28.178	28.276	17.543
24.861	24.885	16.567	28.450	28.545	18.013
24.571	24.597	16.438	28.315	28.408	17.949
23.571	23.596	16.310	27.256	27.349	17.887
22.597	22.622	16.047	26.229	26.323	17.711
21.951	21.973	15.785	25.462	25.557	17.535
21.467	21.485	15.449	24.821	24.918	17.298
20.991	21.005	15.113	24.192	24.289	17.061
20.780	20.789	14.778	23.838	23.936	16.789
20.573	20.578	14.445	23.491	23.589	16.517
20.403	20.404	14.165	23.194	23.292	16.255
20.299	20.296	13.887	22.990	23.089	15.994
20.199	20.193	13.687	22.792	22.890	15.783
20.131	20.121	13.488	22.643	22.742	15.572
20.080	20.068	13.371	22.522	22.621	15.437
20.033	20.018	13.254	22.405	22.504	15.302
20.003	19.987	13.216	22.331	22.430	15.255
19.977	19.960	13.178	22.261	22.359	15.209
19.956	19.937	13.216	22.202	22.300	15.255
19.941	19.921	13.254	22.162	22.260	15.302
19.929	19.909	13.371	22.126	22.224	15.437
19.921	19.900	13.488	22.104	22.203	15.572
19.916	19.895	13.687	22.092	22.190	15.783
19.915	19.894	13.887	22.083	22.181	15.994
19.916	19.895	14.165	22.092	22.190	16.255
19.921	19.900	14.445	22.104	22.203	16.517
19.929	19.909	14.778	22.126	22.224	16.789
19.941	19.921	15.113	22.162	22.260	17.061
19.956	19.937	15.449	22.202	22.300	17.298
19.977	19.960	15.785	22.261	22.359	17.535
20.003	19.987	16.047	22.331	22.430	17.711
20.033	20.018	16.310	22.405	22.504	17.887
20.080	20.068	16.438	22.522	22.621	17.949
20.131	20.121	16.567	22.643	22.742	18.013
20.199	20.193	16.444	22.792	22.890	17.543
20.299	20.296	16.322	22.990	23.089	17.075
20.403	20.404		23.194	23.292	
20.573	20.578		23.491	23.589	
20.780	20.789		23.838	23.936	
20.991	21.005		24.192	24.289	
21.467	21.485		24.821	24.918	
21.951	21.973		25.462	25.557	
22.597	22.622		26.229	26.323	
23.571	23.596		27.256	27.349	
24.571	24.597		28.315	28.408	
24.861	24.885		28.450	28.545	
24.869	24.890		28.178	28.276	
24.973	24.991		27.986	28.089	
			Mean		
21.304	21.305	14.884	24.126	24.223	16.680

Figure 11. The graphical representation of the stresses

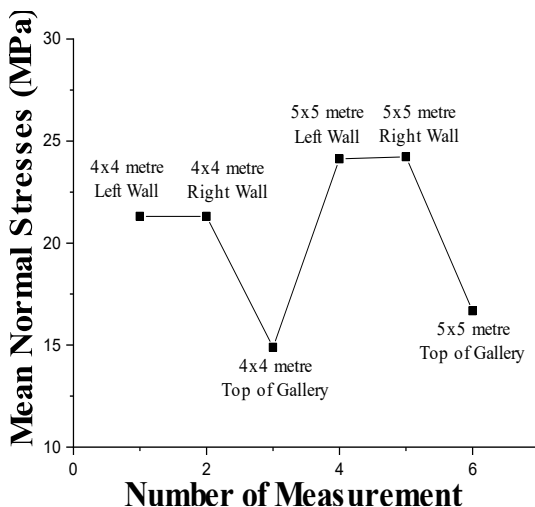


Figure 11. The graphical representation of the stresses

4. RESULTS AND DISCUSSION

In the scope of this study, vertical stresses expected to occur around galleries of different sizes were calculated through two different stress analyzes in the first stage, the vertical and horizontal stresses that would affect the galleries were calculated using the Phase2D program. In the second stage, the ANSYS stress analysis software was used to measure the vertical stress values around the gallery and the deformation and vertical stress values that would occur in the third dimension within the galleries. Because of the stress analyzes conducted in the first stage, it can be observed from the values given in Table 3 that the stresses increase linearly from the base region of the gallery toward the upper region of the gallery. They decrease slightly, stabilizing, and are influenced by the pressure arch formed on the gallery's upper portion. This situation has also been explained in detailed scientific studies on the subject [13-20]. It is noted

that the vertical stresses occurring in the 4×4 meter and 5×5 meter gallery sizes are very close to each other, but the vertical stresses on the gallery's upper portion are particularly lower in the 4×4 meter gallery size.

Looking at the average horizontal stress values around the gallery given in Table 3 because of the first-stage stress analysis, it is observed that the stresses on the left and right walls of the 4×4 meter and 5×5 meter gallery sizes are very close to each other. The lowest average vertical stress value was observed in the upper region of the 4×4 meter gallery size.

Because of the two-stage stress analyzes it was determined that the horizontal stress values occurring in the left and right regions of the gallery are very close to each other. However, especially in the graphical representation shown in Figure 11, it is evident that the normal stresses occurring on the gallery and analyzed in the second and third dimensions are lower in the 4×4 meter gallery size. In addition, it allows for less deformation. Therefore, it has been determined that designing the gallery sizes to be opened in the working area as 4×4 meters would be suitable in terms of both work efficiency and health.

5. CONCLUSIONS

Predicting the behavior of the rock mass in which galleries will be excavated under load is crucial for gallery stability, work efficiency, and safety. Galleries that are excavated in the correct dimensions will result in a more balanced stress distribution, ensuring the stability of the gallery throughout the mining operation. In the scope of this study, galleries designed in sizes of 4×4 meters and 5×5 meters, which are planned to be excavated within the considered rock mass, were analyzed for the stresses occurring around them through three-dimensional analysis.

It is undeniable that three-dimensional models better reflect the mining conditions. According to the obtained results, it was observed that the stresses and vertical deformation values are lower in the 4×4 meter gallery size. Considering the geomechanical parameters of the rock mass and the results of stress analysis, no failure is expected in galleries to be excavated in these dimensions. However, through regular discontinuity control in the field, precautions can be taken to prevent ceiling collapses due to the formation of rock wedges during gallery excavation.

REFERENCES

- [1] He, B., Yin, G.Z. (2014). Stability analysis of tunnel during the excavation based on ANSYS. *Applied Mechanics and Materials*, 577: 1135-1138. <https://doi.org/10.4028/www.scientific.net/AMM.577.1135>
- [2] Fakhimi, A., Carvalho, F., Ishida, T., Labuz, J.F. (2002). Simulation of failure around a circular opening in rock. *International Journal of Rock Mechanics and Mining Sciences*, 39(4): 507-515. [https://doi.org/10.1016/S1365-1609\(02\)00041-2](https://doi.org/10.1016/S1365-1609(02)00041-2)
- [3] Hendron, A.J., Engeling, P.D., Paul, S.L., Aiyer, A.K. (1972). Geomechanical model study of the behavior of underground openings in rock subjected to static loads: Report 3: Tests on lined openings in jointed and intact rock. Technical Report N-69-1. Waterways Experiment Station, Vicksburg, Mississippi, US.
- [4] Huang, F., Zhu, H., Xu, Q., Cai, Y., Zhuang, X. (2013). The effect of weak interlayer on the failure pattern of rock mass around tunnel-scaled model tests and numerical analysis. *Tunnelling and Underground Space Technology*, 35: 207-218. <https://doi.org/10.1016/j.tust.2012.06.014>
- [5] Ren, F., Chang, Y., He, M. (2020). A systematic analysis method for rock failure mechanism under stress unloading conditions: A case of rock burst. *Environmental Earth Sciences*, 79: 1-16. <https://doi.org/10.1007/s12665-020-09111-2>
- [6] Yetkin, M.E. (2022). Metalik Madenlerde Topuk Boyutlarındaki Değişimin Gerilme Dağılımına Etkisi. *Afyon Kocatepe Üniversitesi Fen Ve Mühendislik Bilimleri Dergisi*, 22(6): 1459-1468. <https://doi.org/10.35414/akufemubid.1148884>
- [7] Malli, T., Yetkin, M.E., Özfirat, M.K., Kahraman, B.A. Y.R.A.M. (2017). Numerical analysis of underground space and pillar design in metalliferous mine. *Journal of African Earth Sciences*, 134: 365-372. <https://doi.org/10.1016/j.jafrearsci.2017.07.018>
- [8] RocData. (2014). Rock, Soil and Discontinuity Strength Analysis, Version 5.0. <https://www.roscience.com/software/rsdata#>.
- [9] Sheorey, P.R. (1994). A theory for in Situ stresses in isotropic and transverseley isotropic rock. *International Journal of Rock Mechanics and Mining Sciences & Geomechanics Abstracts*, 31(1): 23-34. [https://doi.org/10.1016/0148-9062\(94\)92312-4](https://doi.org/10.1016/0148-9062(94)92312-4)
- [10] Phase2, Version 8.020. (2014). Rocscience Inc, Toronto, Ontario, Canada. <https://www.roscience.com/software/rs2>.
- [11] SpaceClaim Corporation. (2014). SpaceClaim (2014.0.1.03201), SpaceClaim Corporation. <https://www.ansys.com/products/3d-design/ansys-spaceclaim>.
- [12] Ansys Mechanical. (2018). ANSYS, Inc., Canonsburg PA, USA. <https://www.ansys.com/products/structures/ansys-mechanical>.
- [13] Poulsen, B.A. (2010). Coal pillar load calculation by pressure arch theory and near field extraction ratio. *International Journal of Rock Mechanics and Mining Sciences*, 47(7): 1158-1165. <https://doi.org/10.1016/j.ijrmms.2010.06.011>
- [14] Wang, S.L., Hao, S.P., Chen, Y., Bai, J.B., Wang, X.Y., Xu, Y. (2016). Numerical investigation of coal pillar failure under simultaneous static and dynamic loading. *International Journal of Rock Mechanics and Mining Sciences*, 84: 59-68. <https://doi.org/10.1016/j.ijrmms.2016.01.017>
- [15] Basarir, H., Oge, I.F., Aydin, O. (2015). Prediction of the stresses around main and tail gates during top coal caving by 3D numerical analysis. *International Journal of Rock Mechanics and Mining Sciences*. 76: 88-97. <https://doi.org/10.1016/j.ijrmms.2015.03.001>
- [16] Deng, G., Xie, H., Gao, M. (2023). Fracture mechanisms of competent overburden under high stress conditions: A case study. *Rock Mechanics and Rock Engineering*, 56: 1759-1777. <https://doi.org/10.1007/s00603-022-03169-z>
- [17] Yetkin, M.E., Özfirat, M.K., Onargan, T. (2024). Examining the optimum panel pillar dimension in

- longwall mining considering stress distribution. Scientific Reports, 14(6928): 1-12. <https://doi.org/10.1038/s41598-024-57579-w>
- [18] Kang, H., Wu, L., Gao, F. (2019). Field study on the load transfer mechanics associated with longwall coal retreat mining. International Journal of Rock Mechanics and Mining Sciences, 124: 104141. <https://doi.org/10.1016/j.ijrmms.2019.104141>
- [19] Sinha, S., Walton, G. (2019). Investigation of longwall headgate stress distribution with an emphasis on pillar behavior. International Journal of Rock Mechanics and Mining Sciences, 121: 104049. <https://doi.org/10.1016/j.ijrmms.2019.06.008>
- [20] Li, C.C. (2006). Rock support design based on the concept of pressure arch. International Journal of Rock Mechanics and Mining Sciences, 43(7): 1083-1090. <https://doi.org/10.1016/j.ijrmms.2006.02.007>